5. Effect of treatment by laser irradiation on field emission properties

5.1. Introduction to post-treatment of CNT films

Many efforts have been made to use carbon nanotube for field emission display as a cathode material. Several post treatment methods such as plasma etching, surface rubbing, ion bombardment, and laser irradiation [5.1-5.3] have been employed to modify the characteristics of the CNTs. Takai and co-workers [5.4] have shown that laser irradiation to CNT improves the field emission current. Rinzler [5.5] observed that field emission properties of individual carbon nanotubes were dramatically enhanced by laser irradiation and suggested that the number of emission sites may have been increased by UV laser irradiation in air. Colbert [5.6] has also observed the enhancement of electron emission properties of CNTs after treated with laser irradiation. They attributed this phenomenon to the presence of localized plasma, which is induced by instant vaporization and ionization of the species situated on CNTs. While such an interpretation is in accord with the increase of emission current density after laser irradiation, the existence of localized plasma is somewhat difficult to justify.

The emission of electrons from CNTs has been considered to be from the dangling bonds at the end of CNTs or at the defect sites of CNT body. Therefore irradiating CNTs films with laser beams could have induced defects and/or dangling bonds, resulting in improvement in their emission characteristics In the case of KrF excimer laser, the incident photo energy exceeds the bonding energy of CNT's, bond breaking can possibly result in dangling bonds formation.

The use of laser irradiation, if proved to be viable, is attractive, since it can be easily integrated in a manufacture line, with reasonable through put. In this study, the modifications on the ratio of I_D/I_G resulted from KrF excimer laser irradiation have been investigated. We focus on attention on the influence of laser power density, laser pulse counts, and atmosphere to the improvement of field emission properties. We use a simple environment to demonstrate that it really works and report the results of measurement and the analysis of field emission characteristic, so as to understand the possible modification mechanism involved.

5.2. Experimental detail

CNT films were irradiated by KrF (248nm) excimer laser with power density from 8 to 15 mJ/cm^2 and pulse counts from 2 to 40. The irradiation was carried out in air with the incident laser beam being defocused. The laser fluence used in this study is adjusted to be smaller than the threshold for destructing the CNTs. After laser irradiation, a diode structure was used for electron emission measurements. The anode and cathode were made by ITO glass substrate. Spacer between them was 180 μm and the distance was so small that edge emission could be ignored. The emission characteristics were made in a vacuum chamber under a pressure of 10^{-5} torr. Electrical potential applied to nanotube emitters was typically from 0 to 1100V by Keithely 237 electrometer. Detail about synthesis of nanotubes are listed in Table 5.1.

Table 5.1: *Fabrication process of as-grown nanotubes prepared for post-treatment.*

Pretreament					Growth			
Temperature (^{0}C)	Pressure (torr)	Power (W)	Time (min)	Gas ratio (H_2/sccm)	Power (W)	Time (min)	Gas ratio (H_2/CH_4)	Bias (V)
500	24	800	15	90	1200	10	90:10	0

We discuss the effects of laser irradiation based on the following three parameters:

(1) Dependence on laser power density

(2) Dependence on laser counts

(3) Dependence on the atmosphere during irradiation.

Detail about irradiation conditions of three different treatments were summarized in Table 5.2, Table 5.3, and Table 5.4, respectively.

Table 5.2: *Details of post-treatment process dependence on laser power.*

Sample	Vacuum (torr)	Laser power (mJ)	Laserpower density (mJ/cm^2)	Laserpulse (counts)	Frequency (cm^{-1})
1	virgin	virgin	virgin	virgin	virgin
2	air	27.7	8.87	10	0.2
3	air	44.4	14.10	10	0.2

Table 5.3: *Details of post-treatment process dependence on laser counts.*

Sample	Vacuum(torr)	power(mJ)	Power density (mJ/cm^2)	pulse(counts)	Frequency(cm^{-1})
1	virgin	virgin	virgin	virgin	virgin
2	air	27.7	8.87	2	0.2
3	air	27.7	8.87	5	0.2
4	air	27.7	8.87	10	0.2
5	air	27.7	8.87	30	0.2

Table 5.4: *Details of post-treatment process dependence on atmosphere during irradiation.*

Sample	Vacuum (torr)	Laser power (mJ)	Laserpower density (mJ/cm^2)	Laserpulse (counts)	Frequency (cm^{-1})
1	5E-5torr	28.26	9.06	5	0.2
2	5E-1torr	28.26	9.06	5	0.2
3	760torr	28.26	9.06	5	0.2

5.3. Results and discussion

5.3.1. Dependence of laser power density

Figure 5.1 shows the SEM photos of the CNTs with and without laser irradiation. We can not find much difference between these images. The results suggested that laser irradiation might damage the individual CNT body but not the films morphology.

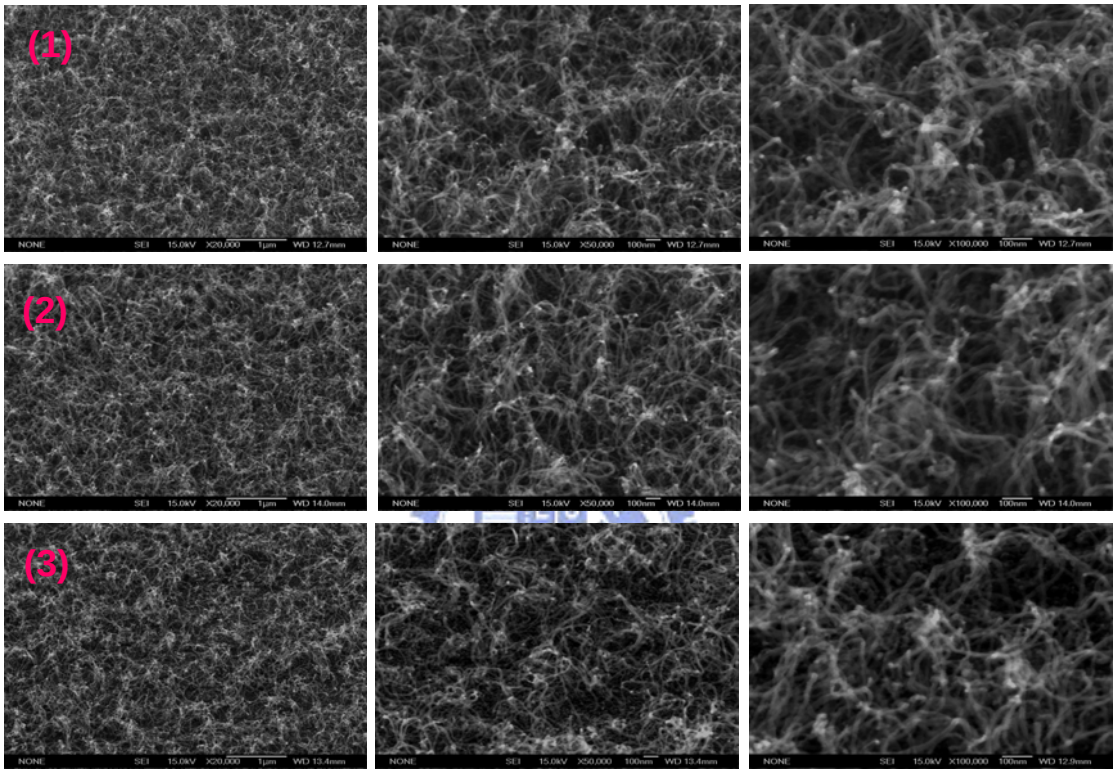

Figure 5.1: SEM photographs arranged in three magnifications of CNTs irradiated with different laser power density; (1) as-grown CNTs, (2)8.87mJ/cm2, and (3) 14.23mJ/cm2.

5.3.1.1. Raman

Figure 5.2 shows the Raman spectra of CNTs with and without laser irradiation and the spectra characteristics were summarized as Table 5.5. Figure 5.2(b) shows that the I_D/I_G increased with the increasing power density, indicating that more dangling bonds and defects sites were created due to increasing laser photon excitation [5.1-5.3]. The lager I_D/I_G ratio, to the zeroth order, indicates poor quality of graphite crystalline.

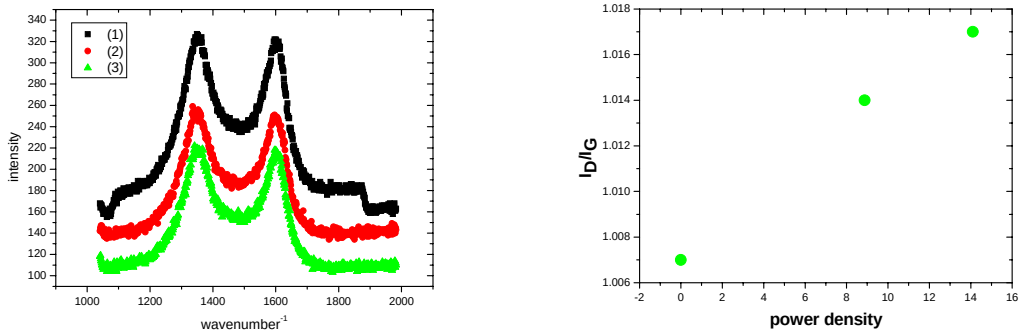

(a) (b)

Figure 5.2: (a) Raman spectra of CNTs irradiated with different laser power density; (1) as-grown CNTs, (2)8.87mJ/cm2, and (3) 14.23mJ/cm2.(b) The ID/IG dependence on power density.

Table5.5: *Characteristic of Raman spectra*

Sample	D band (cm^{-1})	G band (cm^{-1})	I_D	I_G	I_D / I_G
1	1349	1600	284	282	1.007
2	1334	1596	234	231	1.014
3	1341	1596	232	228	1.017

5.3.1.2. FEM

Figure 5.3 shows the I-V characteristics and the F-N plots of CNTs before and after laser irradiation. The emission current increased from 0.98 mA/cm^2 at a applied voltage of 1100V to 2.46 mA/cm^2 at the same applied voltage after laser irradiation with power density 14.10mJ/cm^2 and 10 counts, while the turn-on field decreased from 4.89 to 3.15 V/μm. Characteristics of the I-V measurement were summarized in Table 5.6.

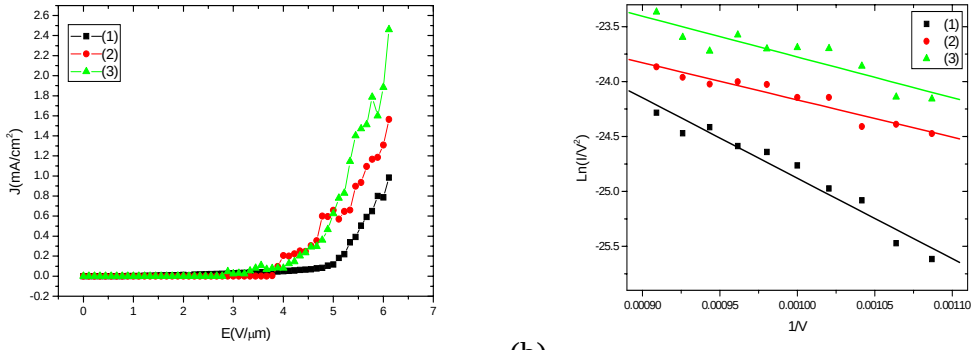

(a) (b)

Figure 5.3: (a)I-V characteristic of nanotubes irradiated with different laser power density; (1) as-grown CNTs, (2)8.87mJ/cm2, and (3) 14.23mJ/cm2, (b) the corresponding F-N plots of the I-V curves.

Table 5.6: *Characteristic of the filed emission characteristics.*

Sample	Turn-on field (J=0.1mA/cm^2) (V/μm)	Current density V=1100 (mA/cm^2)	Field enhancement dactor(β)
1	4.89	0.98	1932
2	3.88	1.56	4759
3	3.55	2.46	2668

Figure 5.4 shows the I_D/I_G dependence on field emission performance. The increasing I_D/I_G results in the decreasing turn-on field (a) and increasing current density (b). Both these effects improved the field emission properties. On the other hand, there is no strong correlation between I_D/I_G and beta.

(a) (b)

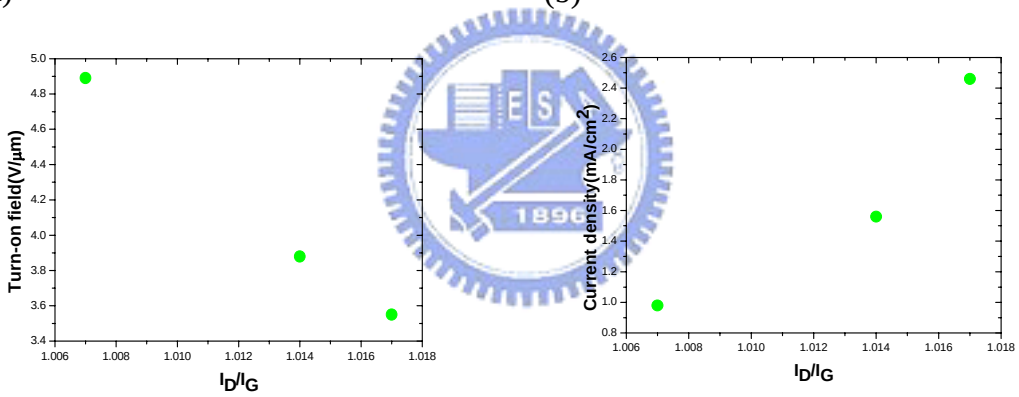

(c)

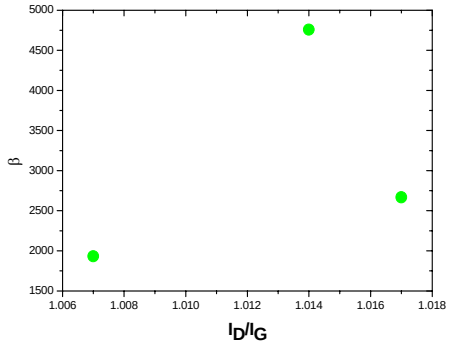

Figure 5.4: The I_D/I_G dependence on field emission properties; (a) Turn-on field, (b) Current density, and (c) Enhancement factor.

5.3.2. Dependence of laser counts

Figure 5.5 shows the morphology of the CNTs before and after laser irradiation. It is clear that there was no obvious difference observed from these images, as we have seen in preceding section. The same observation applies to both two experiments. It is emphasized that the difference due to incident photons might be macroscopic(morphology and distribution) but microscopic(graphite structure of CNT body).

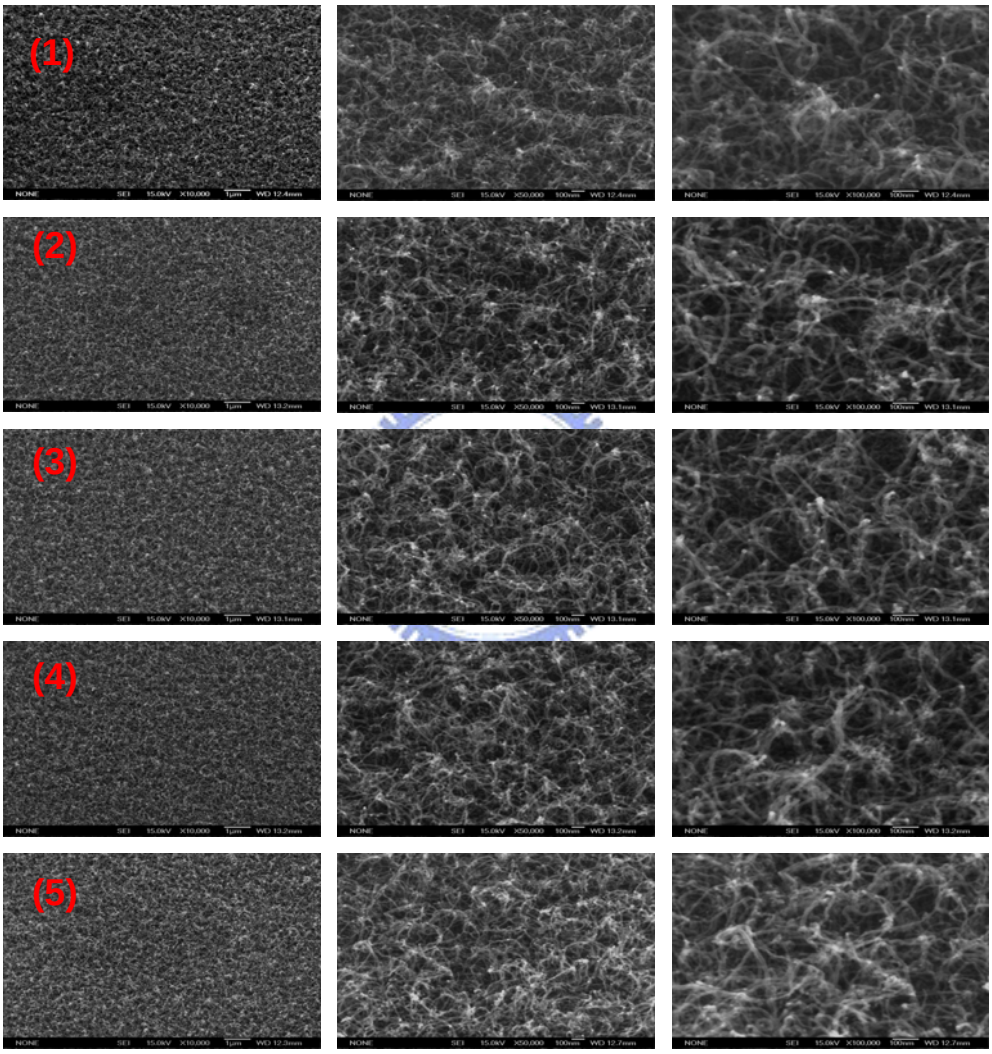

Figure 5.5: SEM photographs of CNTs irradiated with different laser counts; (1) as-grown CNTs, (2) counts=2, (3) counts=5, (4) counts=10, and (5) counts=30.

Figure 5.6 shows the Raman spectra of CNTs before and after laser irradiation and the spectra characteristics are summarized as Table 5.7. Figure 5.6(b) shows that more incident laser counts resulted in more damages (reflected in the increasing I_D/I_G ratio). Our results agree with those reported by M.Takai [5.4].

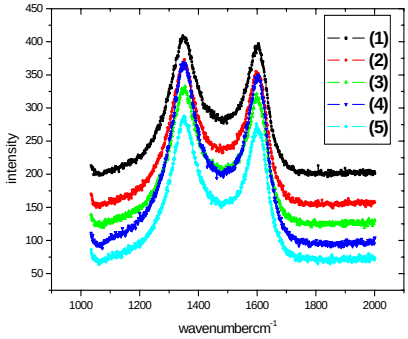

(a)

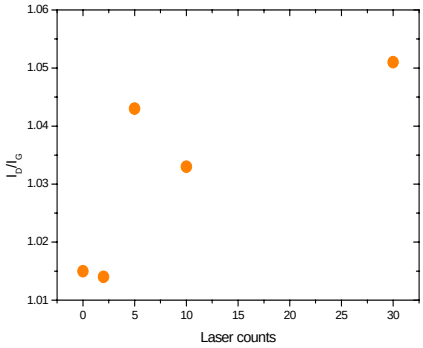

(b)

Figure 5.6:(a) Raman spectra of nanotubes of CNTs irradiated with different laser counts; (1) as-grown CNTs, (2) counts=5, (3) counts=10, (4) counts=20, and (5) counts=30.(b) The ID/IG dependence on laser counts.

Table5.7: *Characteristic of Raman spectra*

Sample#	D band(cm^{-1})	G band(cm^{-1})	I_D	I_G	I_D / I_G
1	1346	1605	334	329	1.015
2	1354	1596	695	629	1.104
3	1353	1596	353	335	1.053
4	1355	1598	342	331	1.033
5	1353	1597	347	336	1.051

Figure 5.7 are the I-V curves and the corresponding F-N plots for the laser irradiation treated CNTs discussed above. The emission current was 0.7 mA/cm^2 at a applied voltage of 1100V and increased to 1.84 mA/cm^2 at the same applied voltage after laser irradiation with power density 8.87mJ/cm^2 and 5 counts. Similar to the previous results, the turn-on field reduced from 5.22 to 2.88 V/μm. It appears that more laser counts would cause more improvement in electron emission. Characteristics from measurements were summarized in Table 5.8.

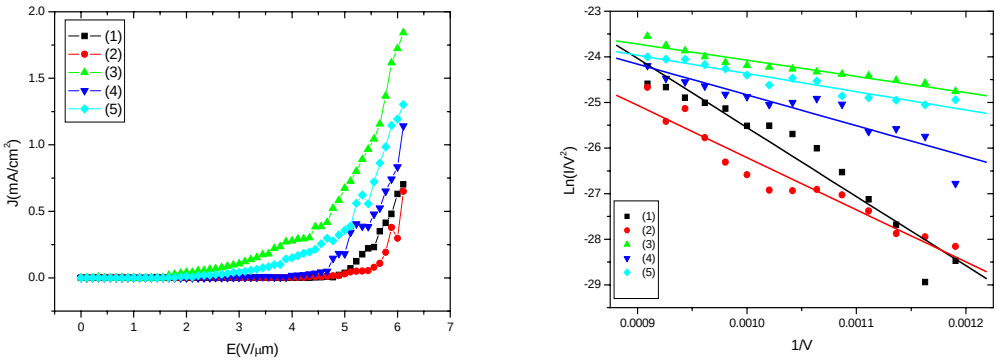

Figure 5.7: I-V characteristic of nanotubes irradiated with different laser counts; (1) as-grown CNTs, (2) 2counts, (3) 5counts, and (4) 10counts, and (5) 30counts, (b) The corresponding F-N plots of the I-V curves.

Table5.8: *Characteristic of field emission properties.*

Sample #	Turn-on field(J=0.1mA/cm^2)(V/μm)	Current density(V=1100)(mA/cm^2)	Field enhancement factor(β)
1	5.22	0.7	905
2	5.66	0.65	1470
3	2.88	1.84	4299
4	4.77	1.14	1733
5	3.66	1.30	3987

Figure 5.8 shows the I_D/I_G dependence on the three field emission properties. We could see that unlike the previous modifications with either bias voltage or added gases, where the microstructure and film morphology may have changed simultaneously, the laser irradiation treatment is more viable in modifying I_D/I_G ratio and the correlation between I_D/I_G ratio and emission performance is more clearly demonstrated.

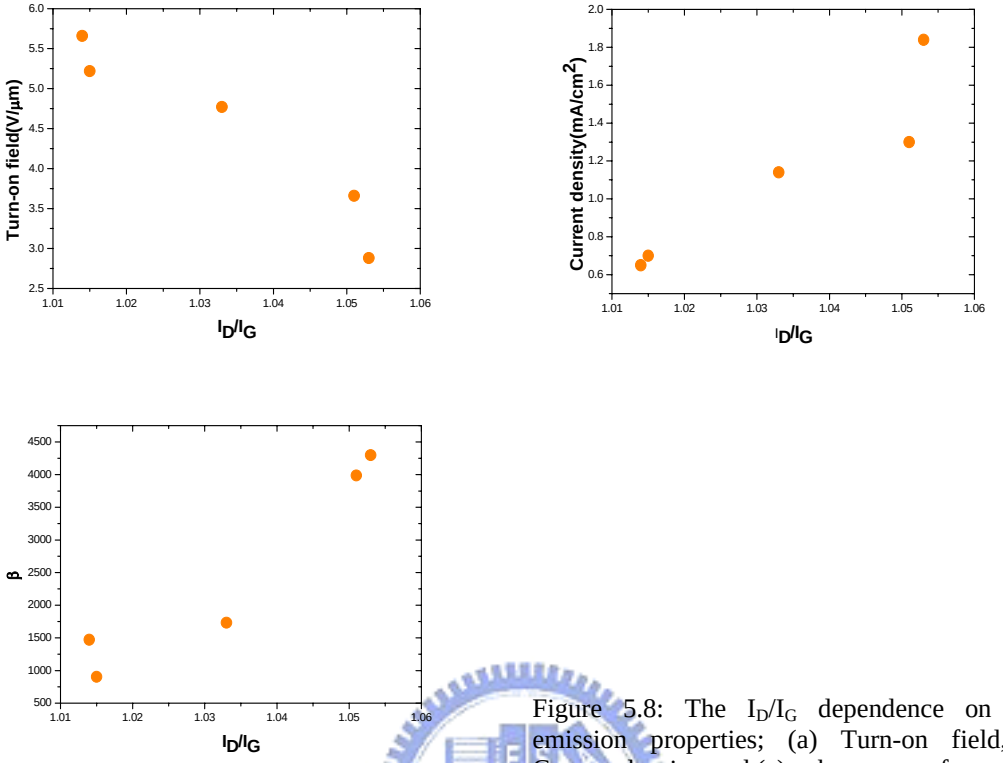

Figure 5.8: The I_D/I_G dependence on field emission properties; (a) Turn-on field, (b) Current density, and (c) enhancement factor.

5.3.3. Dependence on the atmosphere during irradiation

Figure 5.9 shows the morphology of the CNTs with laser irradiation at different atmospheres. The same observation was obtained that the influence of irradiation could not be observed from the morphology images.

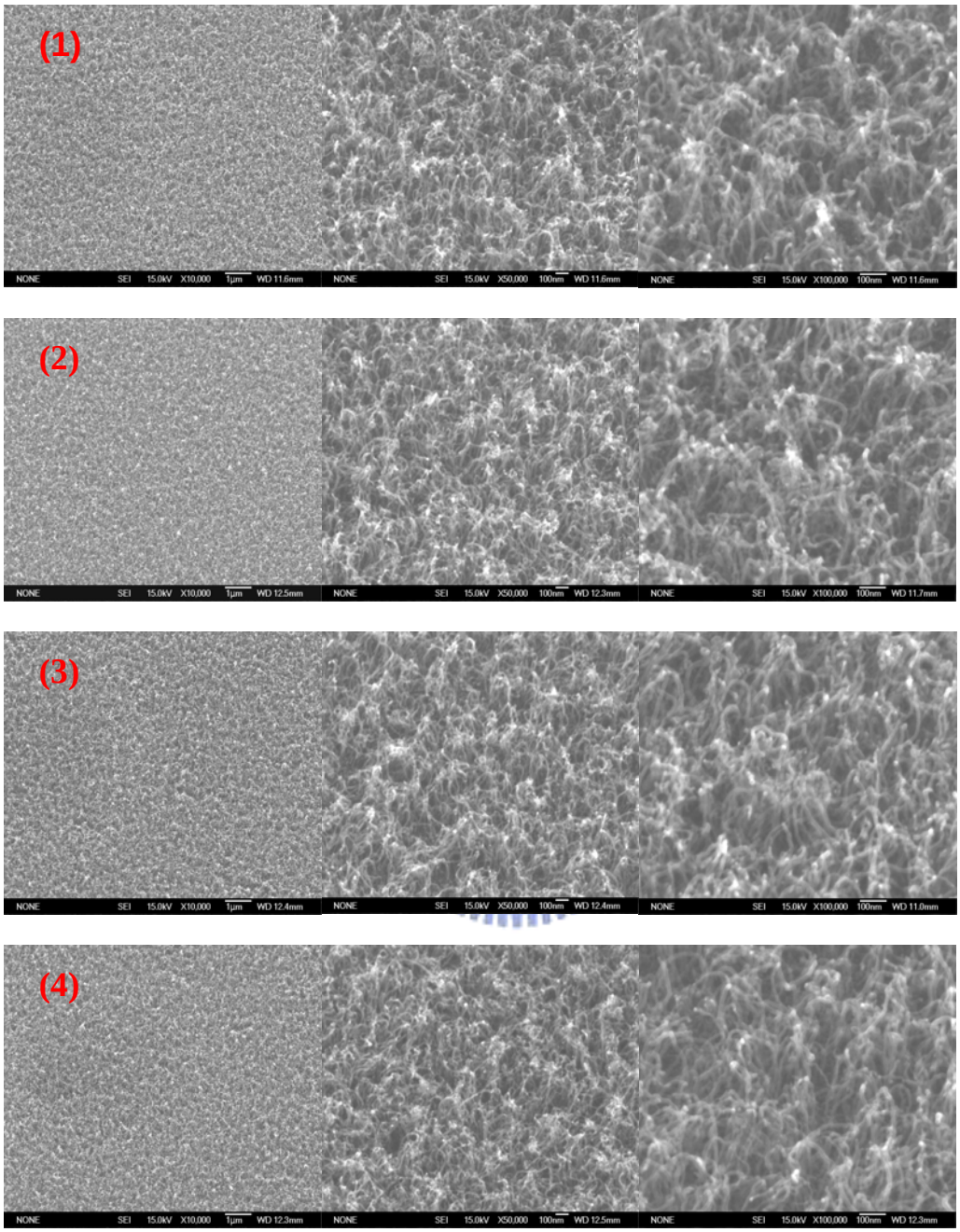

Figure 5.9: SEM images as function of oxygen pressure during irradiation; (1) As-grown CNTs (2) 5E-5torr, (3) 5E-1torr, and (4) 760torr.

5.3.3.1. Raman

Figure 5.10(a) shows the Raman spectra of the CNTs with laser irradiation at different atmosphere and the characteristics were summarized in Table 5.9. Two information could be read from the Figure 5.11(b). First, all the values of I_D/I_G (1.143, 1.131, and 1.105) of the CNTs irradiated were lager than without irradiation (1.007). That means

irradiation by laser cause damage to the CNTs in large range of atmosphere from high vacuum (5E-5torr) to atmospheric condition (760 torr). Secondly, the level of damage decreased with the slightly increased oxygen pressure. This could be that more oxygen burns out more amorphous carbon and the heat arising from inflammation bring about the annealing effect to make crystallite structure better [5.3]. However, further increase of oxygen partial pressure, may, again, over damage the CNT structure.

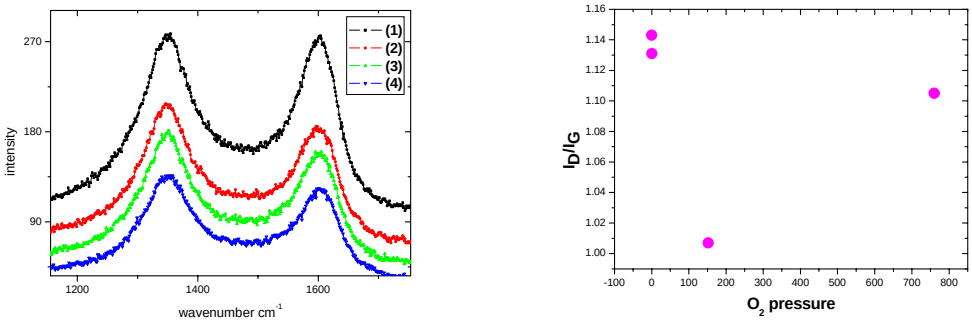

Figure 5.10: Raman spectra of nanotubes as function of oxygen pressure during irradiation; (1) As-grown CNTs (2) 5E-5torr, (3) 5E-1torr, and (4) 760torr.

Table 5.9: *Characteristic of Raman spectra*

Sample	D band (cm^{-1})	G band (cm^{-1})	I_D	I_G	I_D / I_G
1	1351	1603	253	251	1.007
2	1346	1598	183	160	1.143
3	1352	1605	181	160	1.131
4	1346	1597	136	123	1.105

5.3.3.2. FEM

Figure 5.11 shows I-V measurement and F-N plots of the CNTs with laser irradiation at different atmosphere. The current density (@V=1100) of CNTs without irradiation is 2.62mA/cm^2. After irradiation with different oxygen pressure, the current densities were 1.23, 0.92, and 0.39 mA/cm^2, corresponding to oxygen pressure of 5E-5torr, 5E-1torr, and 760torr, respectively. The same results were also observed in other field emission property. Turn-on voltage of CNTs without irradiation was 4.33V/μm and those of irradiation were 4.66 V/μm, 5 V/μm, and 5.55 V/μm, corresponding to different oxygen pressure of 5E-5torr, 5E-1torr, and 760torr, respectively. Details

about field emission properties were listed in Table 5.10.

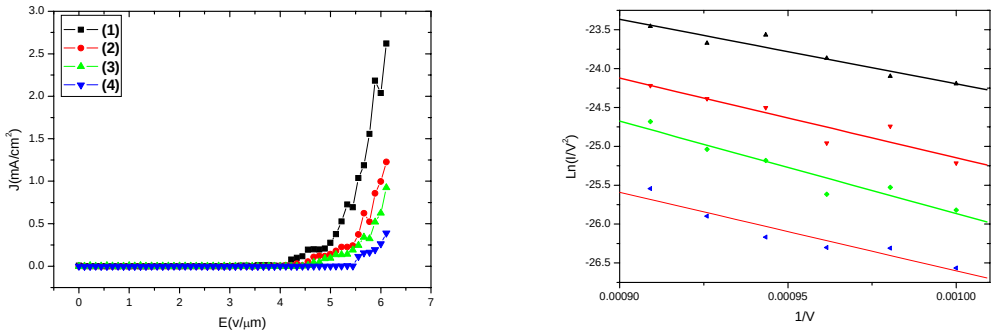

Figure 5.11:(a)I-V characteristic of nanotubes as function of oxygen pressure during irradiation; (1) As-grown CNTs (2) 5E-5torr, (3) 5E-1torr, and (4) 760torr, (b) The corresponding F-N plots of I-V curves.

Table 5.10: *Characteristic of field emission properties*.

Sample	Turn-on field (J=0.1mA/cm^2) (V/ μ m)	Current density V=1100 (mA/cm^2)	Field enhancement dactor(β)
1	4.33	2.62	1657
2	4.66	1.23	1342
3	5	0.92	1156
4	5.55	0.39	1358

Figure 5.12 shows the I_D/I_G dependence on field emission properties. It is seen from Figure 5.12(a) that turn-on field decrease with the increasing I_D/I_G and current density increased with the increasing I_D/I_G (Figure 5.12(b)). No strong correlation was found in the dependence on beta. This indicates that mechanism beta involved was more complicated. More factors need to be concerned when the emitters were films rather than isolated CNT clusters.

(a)

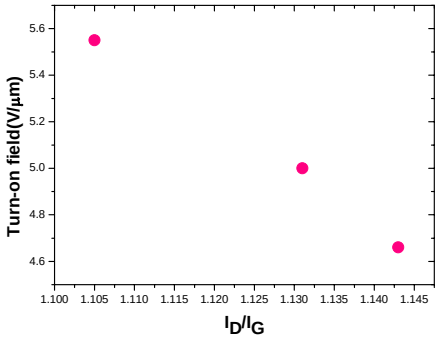

(b)

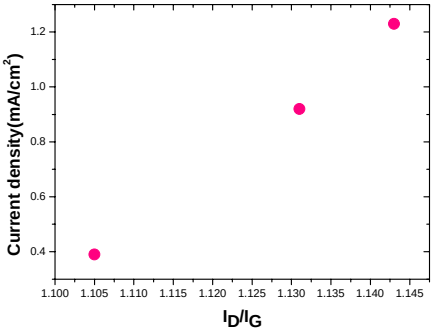

(c)

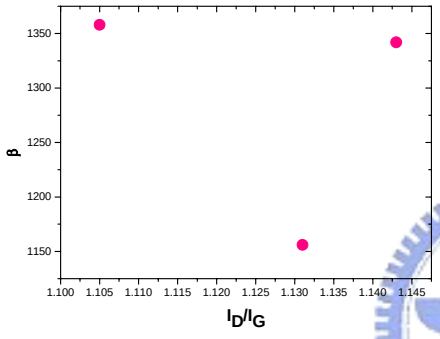

Figure 5.12: The I_D/I_G dependence on field emission properties; (a) Turn-on field, (b) Current density, and (c) enhancement factor.

5.4. The effect of defects on field emission property

Figure 5.13 show the high resolution transmission electron microscopy images before and after laser irradiation, respectively. The red arrows designate the initial wall structure of the as-grown CNTs body and the blue arrows designate the wall structure of those after laser irradiation. The former seems to have more complete wall structures as compared to the latter. We believe that the bombardment of photons would break the bonding between the carbon atoms and cause damage to the structure [5.1-5.3]. The broken regions can be regarded as new emission sites for electron emissions under external applied field.

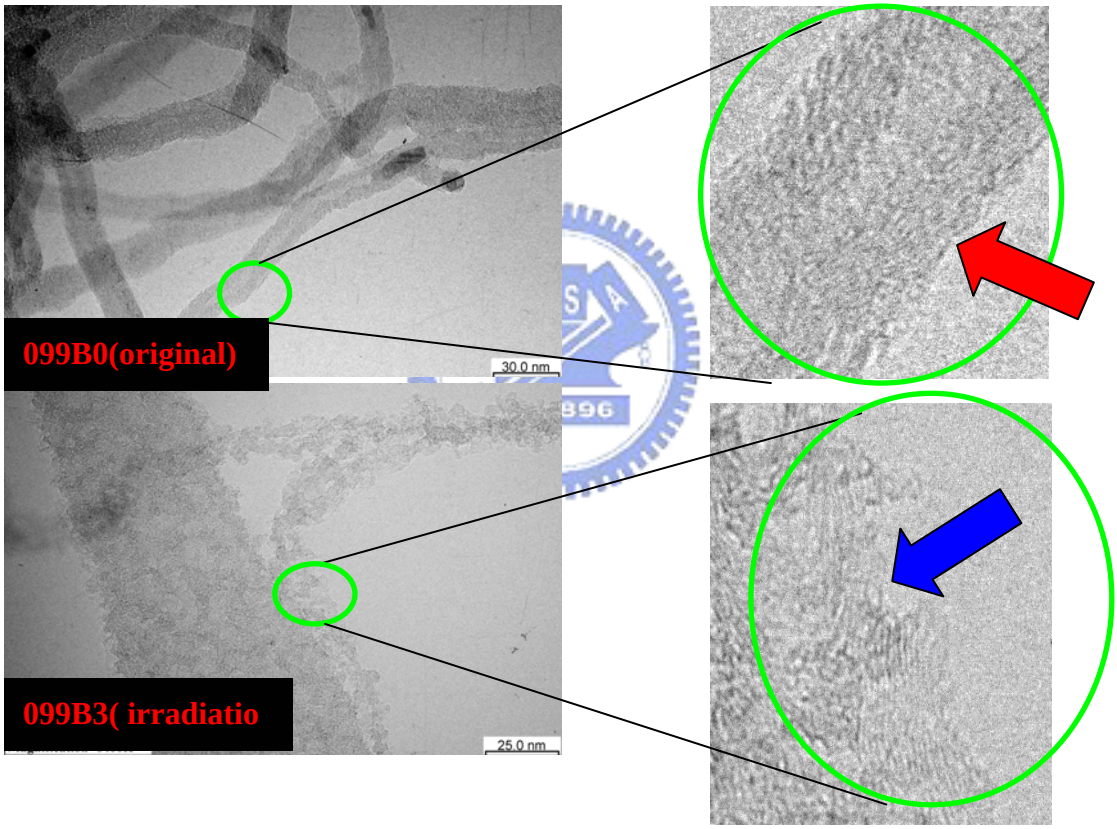

Figure 5.13: HRTEM images of carbon nanotubes with and without laser irradiation. The red arrow indicates the structure of the as-grown CNTs and the blue one indicates the structure damage of CNTs caused by irradiation with KrF excimer laser.

5.5. Conclusion

Results obtained in this section are summarized as follows:

(1) Post-treatment by KrF excimer laser was proved to be practicable to improve the field emission properties of CNT films. The emission current increased by a factor of 2~3 with optimize power density. The turn–on field for CNTs emitters was found to decrease from 4.89-5.22 to 2.88-3.15 V/μm with optimize laser counts. Effect of oxygen pressure during irradiation was found to degrade the performance of field emission properties. The improvement in the emission characteristic induced by the irradiation could be mainly due to the photo-excitation effect such as photo deposition or photo-oxidation [5.2-5.5] rather than the photo-thermal effect.

(2) Modifying I_D/I_G ratio by post-treatment using KrF excimer laser irradiation reveals a strong relationship between I_D/I_G and field emission performance. The decreasing of the ratio reflected the degenerating of the graphite structure [5.4-5.6]. When CNTs films with the same morphology but different ratio of I_D/I_G, the field emission performance was mainly influenced by the graphite structure, which reflected on I_D/I_G ratio.

(3) The TEM images provide a evidence for our suggestion. The mechanism involved in accounting for the β-factor is more complicated and much still remains to be done in the future [5.10-5.11].

Reference

[5.1] A. Sawada, M. Iriguchi, W, J. Zhao, C. Ochiai, and M. Takai, J.Vac.Sci.Technol.B 21, 362(2002).

[5.2] W. Zhao, A. Sawada, and M. Takai , Jpn. J. Appl Phys. 41,4314(2002).

M. Takai, W. J, Zhao, A. Sawada, A. Hosono and S. Okuda, Society for information display[SID] ,Digest of technical papers, Baltimore, 794(2003).

[5.3] W. J. Zhao, N. Kawakami, A. Sawada, and M. Takai, J. Vac. Sci. Technol.B 21, 1734(2003).

[5.4] W. J. Zhao, N. Kawakami, A. Sawada, and M. Takai, J. Vac. Sci. Technol. B 21, 1734 (2003).

[5.5] D. T. Colbert, R. E. Smally, Carbon 33, 921 (1995).

[5.6] Y. Gotoh, Y. Kawamura, K. Ishizu, H. Tsuji, and J. Ishikawa, Proceedings of 11th International Display Workshops, 1209(2005)

[5.7] K. Murakami, W. Rochanachirapar, N. Yamasaki, S. Abo, F. Wakaya, M. Takai, A. Hosono and S.Okuda, Proceedings of 11th International Display Workshops, 1201 (2005).

[5.8] F. Tuinstra and J. L. Koenig, J. Chem. Phys. 53, 1126 (1970)

[5.10] Diamond Relat. Mater.11(2002)763-768

[5.11] D. Y. Zhong, G. Y. Zhang, and S. Liu, Applied Physics Letters, 80, 506(2002).